

In vivo time-resolved autofluorescence measurements to test for glycation of human skin

Jennifer Blackwell

Kamal M. Katika

Laurent Pilon

University of California, Los Angeles
Mechanical and Aerospace Engineering Department
Los Angeles, California 90095

Katrina M. Dipple

University of California, Los Angeles
Departments of Human Genetics and Pediatrics
David Geffen School of Medicine
Los Angeles, California 90095

Seymour R. Levin

Aksone Nouvong

Greater Los Angeles Healthcare System
Department of Veterans Affairs
Los Angeles, California 90073
and

University of California, Los Angeles
Departments of Medicine and Surgery
David Geffen School of Medicine
Los Angeles, California 90095

Abstract. We present an evaluation of time-resolved fluorescence measurements on human skin for screening type 2 diabetes. *In vivo* human skin is excited with a pulse diode at 375 nm and pulse width of 700 ps. Fluorescence decays are recorded at four different emission wavelengths: 442, 460, 478, and 496 nm. Experiments are performed at various locations, including the palms, arms, legs, and cheeks of a healthy Caucasian subject to test single-subject variability. The fluorescence decays obtained are modeled using a three-exponential decay. The variations in the lifetimes and amplitudes from one location to another are minimal, except on the cheek. We compare the fluorescent decays of 38 diabetic subjects and 37 nondiabetic subjects, with different skin complexions and of ages ranging from 6 to 85 yr. The average lifetimes for nondiabetic subjects were 0.5, 2.6, and 9.2 ns with fractional amplitudes of 0.78, 0.18, and 0.03, respectively. The effects of average hemoglobin A1c (HbA1c) from the previous 4 yr and diabetes duration are evaluated. While no significant differences between the fluorescence lifetimes of nondiabetic and diabetic subjects are observed, two of the fractional amplitudes are statistically different. Additionally, none of the six fluorescence parameters correlated with diabetes duration or HbA1c. One of the lifetimes as well as two of the fractional amplitudes differ between diabetic subjects with foot ulcers and nondiabetic subjects. © 2008 Society of Photo-Optical Instrumentation Engineers. [DOI: 10.1117/1.2830658]

Keywords: skin autofluorescence; time-resolved fluorescence; advanced glycated end-products; diabetes; foot ulcers.

Paper 06378RR received Dec. 21, 2006; revised manuscript received Oct. 9, 2007; accepted for publication Oct. 10, 2007; published online Feb. 29, 2008. This paper is a revision of a paper presented at the SPIE conference on Photonic Therapeutics and Diagnostics II, Jan. 2006, San Jose, Calif. The paper presented there appears (unrefereed) in SPIE Proceedings Vol. 6078.

1 Introduction

Fluorescence is the physical phenomenon in which light is emitted by a substance as a result of excited electrons returning to their ground states after absorption of excitation light. Biological tissues contain several endogenous fluorophores such as nicotinamide adenine dinucleotide (NADH), aromatic amino acids such as tryptophan, and structural proteins including collagen and elastin.¹ The optical properties of these fluorophores respond to the environment and metabolic status of the tissue, thus making fluorescence spectroscopy a valuable tool to study the state of biological tissues. Fluorescence spectroscopy consists of measuring the fluorescent intensity emitted by fluorophores after being excited by light at a suitable wavelength and can be performed in either a steady-state or a time-resolved manner.

Steady-state measurements typically involve measuring either the fluorescence intensity over a range of wavelengths for a fixed excitation wavelength (emission spectra) or the fluo-

rescence intensity at a particular wavelength for a range of excitation wavelengths (excitation spectra). Time-resolved measurements consist of measuring the lifetime of the fluorophores and are much more complex than steady-state spectral measurements due, in part, to the instrumentation required. Steady-state measurements are relatively easy to perform. However, they present some limitations. First, they are intensity dependent and therefore are sensitive to excitation light intensity, optical losses in the experimental setup, and absorption and scattering by tissue.² Second, the fluorescence intensity is integrated over time and, therefore, information associated with the dynamics of the fluorescence process is lost. Time-resolved measurements, on the other hand, capture the transient decay, which depends on the relative concentrations and lifetimes of the fluorophores contributing to the fluorescence signal.² They are also extremely sensitive to the local biochemical environment such as the pH and oxygenation, which may differ in healthy and diseased tissue.² In addition, the fluorophore lifetimes are independent of absolute intensity and so do not change with variations in excitation intensity or optical losses from hemoglobin absorption.² Finally, fluo-

Address all correspondence to Laurent Pilon, UCLA Dept. of Mechanical and Aerospace Engineering, 420 Westwood Plaza, 37-132 Engineering IV, Los Angeles, California 90095-1597; Tel: 310-206-5598; Fax: 310-206-2302; E-mail: pilon@seas.ucla.edu

cence lifetime measurements enable the discrimination of fluorophores with overlapping emission spectra but different lifetimes.³ For example, various tryptophan residues in proteins have similar emission spectra but different lifetimes and thus can be distinguished by time-resolved fluorescence measurements.⁴

Time-resolved fluorescence techniques can be performed in either the frequency domain or the time domain.⁴ Frequency-domain techniques involve exciting the sample with a sinusoidally modulated source, which could be a continuous wave laser or a flash lamp, and measuring⁴ the phase shift of the emitted light at multiple excitation frequencies to compute the fluorescence lifetime(s). Alternatively, time-domain measurements typically use ultrashort pulsed light to excite the sample and measure the emitted fluorescence as a function of time, thus enabling one to compute the lifetime of the fluorophore. Note that the pulse width must be of the same order of magnitude as or shorter than the fluorescence lifetime. Time-domain measurements are preferred in a clinical setting, because they can be obtained in short acquisition times compared to frequency-domain measurements³ and they are not affected by ambient light at the collection site.³

The detection of the diabetic state has become an important issue recently as the number of people with diabetes is rising and approximately one-third of people affected by type 2 diabetes in the United States are undiagnosed.⁵ The current methods of diagnosis consist of detecting glucose levels in the blood or plasma.⁶ Even with screening, the sensitivity is much less than ideal.⁷ Once diabetes has been diagnosed, glucose levels and hemoglobin A1c (HbA1c) are currently utilized to follow the efficacy of treatment. The latter is a measure of percent glycated hemoglobin and reflects average glycemic control over the antecedent 3 to 4 months.⁸ As a test of short-term glycation, HbA1c does not adequately reflect the accumulation of glycated tissue over a period of years, which may result in diabetic complications. To directly measure tissue glycation, a punch biopsy must be taken,⁹ making it difficult to determine a patient's risk for complications. Thus, a simple, rapid method of screening is being pursued to enable early diagnosis of the disease and to follow the efficacy of therapy and the effects of long-term hyperglycemia on tissue.

Spectroscopy-based methods are attractive for diabetes screening and monitoring because they can noninvasively detect some markers of disease progression. For example, the accumulation of advanced glycation end-products (AGEs) in tissue can potentially be observed via spectroscopy. AGEs are the final products of the complex chemical reaction, known as the Maillard reaction, between sugars such as glucose and proteins, lipids, and nucleic acids.⁹ While the accumulation of these in tissues is a natural process and serves as a marker of aging,¹⁰ elevated blood glucose levels in diabetic individuals results in a more rapid accumulation of AGEs. Some AGEs, such as pentosidine, are known to fluoresce and their fluorescence spectra are well characterized.¹¹ It has also been established that the steady-state autofluorescence of skin is correlated with age.¹⁰ Additionally, the formation of these AGEs produces structural changes in tissue proteins, such as collagen,¹² which can be detected through spectroscopy measurements.¹³

This study evaluated the use of a time-resolved fluorescence device using time-correlated single-photon counting

(TCSPC) on *in vivo* human skin to screen for type 2 diabetes. An additional goal of this study was to evaluate the use of the time-resolved fluorescence device to assess a patient's risk for complications based on changes in skin fluorescence caused by AGE formation. Preliminary experiments were performed on the palms, arms, feet, and cheeks of a 31-year-old Caucasian subject to observe measurement variability due to testing location. The device was tested on 37 healthy and 38 diabetic subjects of different age, gender, and skin, complexion after obtaining informed consent and approval from University of California, Los Angeles (UCLA) and Veteran's Administration (VA) institutional review boards. The study refers to "healthy subjects" as those who are not known to be diabetic, and "diabetic subjects" as those who have been diagnosed with diabetes. Variability in recovered time-resolved fluorescence parameters due to age, skin color, and gender was also tested. Also, 18 diabetic subjects with foot ulcers were compared with 18 age-matched healthy subjects to test for differences due to the development of complications. Finally, the possible origin of these fluorescence lifetimes is discussed. This is the first study to report the application of time-resolved fluorescence to the detection of diabetes and/or monitoring for the development of diabetic complications. This work is of particular importance to studies on skin autofluorescence measurements for noninvasive glucose sensing¹⁴ and the design of implantable glucose sensors based on fluorescence.¹⁵ It would also serve as a baseline for using time-resolved autofluorescence of human skin to monitor other diseases and conditions such as skin cancer, wounds, and ulcers.

2 Current State of Knowledge

2.1 Time-Resolved Fluorescence Measurements on Tissue

In vivo time-resolved fluorescence measurements have come into prominence only recently and a limited number of studies have been reported in the literature, which is summarized in Table 1. For example, Pradhan et al.¹⁶ used fluorescence lifetime measurements to study breast tissue. They made use of laser pulses of 100 fs pulse width at 310 nm and a streak camera to obtain a 2-D map of the fluorescence lifetimes. It was shown that time-resolved fluorescence measurements at an emission wavelength around 340 nm can be used to distinguish malignant tumors from nonmalignant breast tissues.

Fluorescence lifetime measurements have also been used to study tissue during endoscopy. Glanzmann et al.¹⁷ described a time-resolved fluorescence instrument based on pumped laser excitation sources and a streak camera coupled to a spectrograph as a detector. The instrument was used to measure the fluorescence decays of endogenous fluorophores and of δ -aminolevulinic acid (ALA)-induced protoporphyrin IX (PPIX) in an excised human bladder with carcinoma. The authors were able to correctly distinguish healthy tissue, which appeared abnormal in steady-state spectroscopy, from cancerous tissue. The instrument was then used to perform *in situ* characterization during endoscopy to obtain time-resolved spectra of tissue fluorescence of human bladder, bronchi, and esophagus.¹⁸ Further studies were conducted by the same group¹⁹ to test the viability of fluorescence lifetime as a new contrast parameter between normal and malignant tissue in

Table 1 Experimental studies of time-resolved fluorescence spectroscopy on human tissues.

Reference	Excitation Wavelength (nm)	Emission Wavelength (nm)	Spectroscopy Method	Sensing Region	<i>In Vivo/ in vitro</i>
2	337.1	N.A.	time domain using an avalanche photodiode (APD) and fast oscilloscope	human skin	<i>in vivo</i>
16	310	340 and 440	time domain using a streak camera	breast tissue	<i>in vitro</i>
17	337.1, 425, 476, 500	500–680	time domain using a streak camera	human bladder	<i>in vitro</i>
18	337.1, 480	375–515, 525–615	time domain using a streak camera	bladder, bronchii, esophagus	<i>in vivo</i>
19	406	430–680	time domain using a streak camera	bronchii	<i>in vivo</i> , endoscopy
20	514.5	550–650	frequency domain	bronchii	<i>in vivo</i> , endoscopy
21	337, 400	550	time domain using a gated intensified diode array	esophagus	<i>in vivo</i> , endoscopy
22–24	446	510–700	time domain using TCSPC	human ocular fundus	<i>in vivo</i>
25,26	337.1	370–510	time domain using a transient digitizer	aorta, and its components	<i>in vitro</i>
27,28	405	N.A.	time domain using time gating	skin tumors	<i>in vitro</i>
29	415	N.A.	time domain using time gating	rabbit knee joint and human tooth	<i>in vitro</i>
30–32	750–850	N.A.	time domain using TCSPC	human skin	<i>in vivo</i>

the bronchi. However, they were unable to obtain a contrast in the fluorescence lifetime or the spectrum between normal and moderately dysplastic tissue in the spectral region between 510 and 650 nm. Mizeret et al.²⁰ also studied the feasibility of performing endoscopic fluorescence lifetime measurements using frequency modulation techniques in real time in a clinical setting. The instrument made use of an excitation source at 514.5 nm and a detection unit consisting of CCD units with image intensifier tubes. Fluorescence lifetime values for healthy bronchial tissue were reported. Pfefer et al.²¹ also performed *in vivo* fluorescence lifetime and spectral measurements on patients undergoing routine endoscopic surveillance for Barrett's esophagus. A time-domain instrument consisting of a laser pulsing at 337 nm with a pulse width of 3 ns and an APD coupled to an oscilloscope was used in the experiments. The excitation wavelengths used were 337 and 400 nm and the emission was collected around 550 nm. Results showed that low-risk tissue and high-grade dysplasia could not be differentiated based on the observed data.

Furthermore, Schweitzer et al.^{22,23} performed fluorescence lifetime studies on the human ocular fundus. They made use of TCSPC techniques with a pulsed laser of 300-ps pulse width at a wavelength of 457.9 nm and various emission wavelength ranges. They obtained a lifetime of 1.5 ns in the parapapillary region of the eye and a lifetime of 5 ns in the

optical disc, which they attributed to collagen. They also showed that breathing 100% oxygen affects the fluorescence lifetimes and speculated that the lifetime of fluorophores present in the retinal pigment epithelium depends on the oxygen supply.

Fluorescence lifetime measurements have also been performed on tissue *in vitro*. For example, Maarek et al.²⁵ used time-domain *in vitro* fluorescence lifetime measurements and spectroscopy for diagnosis of atherosclerotic lesions. The instrument consisted of an excitation laser at 337 nm and a pulse width of 3 ns, a microchannel plate photomultiplier attached to a monochromator and connected to a digital oscilloscope. Fluorescence lifetimes were measured at emission wavelengths ranging from 370 to 510 nm. The authors were able to discriminate between stable and unstable lesions by studying the time-resolved spectra of components present in the arterial wall, namely, structural proteins such as collagen, lipoproteins, and cholesterol.²⁶

Moreover, Cubeddu et al.^{27,28} used fluorescence lifetime imaging (FLIM) to study tumors in human skin. The instrumentation consisted of a dye laser pulsing at 405 nm at a pulse width of less than 1 ns and a gated imaging system. An exogenous marker was used to induce selective accumulation of PPIX in proliferative tissue. Tumors were identified using lifetime imaging due to the longer fluorescence lifetime

of PPIX (18 ns) compared to that of healthy tissue (~10 ns). Siegel et al.²⁹ also used FLIM techniques, utilizing a pulsed laser at 415 nm and a pulse width less than 100 fs and a gated optical intensifier to image the autofluorescence from various biological tissue *in vitro*, such as animal tissue, knee joints, and human teeth. Using this instrument they were able to distinguish between tendon, bone, and surrounding tissue, which was not otherwise possible with white light and steady-state fluorescence measurements. Similarly, they showed that various regions in an extracted human tooth can be clearly distinguished using FLIM unlike reflectance and steady-state fluorescence measurements.

Other studies have performed time-resolved fluorescence measurements on human skin. Konig et al.,³⁰ Konig and Riemann,³¹ and Riemann et al.³² used 3-D autofluorescence lifetime imaging and investigated various tissues of patients with psoriasis, nevi, dermatitis, basalioma, and melanoma *in vitro* as well as the skin of healthy subjects *in vivo*. Their system was able to achieve a subcellular spatial resolution and a temporal resolution of 250 ps. The authors analyzed the fluorescence decays from images obtained at various depths of the skin and reported lifetimes of around 1.85 ns at the stratum corneum and a lifetime of about 2.4 ns at a depth of 50 μm within the stratum spinosum. The same group also reported using multiphoton imaging of skin at an excitation wavelength of 740 nm with a 150-ps resolution.³³ A biexponential fit was used to recover a fast lifetime of 0.4 ns and a slow lifetime of 2.4 ns at the stratum spinosum in the epidermis. Additionally, Pitts and Mycek² described a time-domain instrument with both spectral and temporal resolution to measure fluorescence lifetimes and emission spectrum *in vivo* and *in vitro*. The instrument was based on a pumped dye laser with a pulse width of 4 ns as an excitation source and an APD along with a 1-GHz oscilloscope as a detector. Fluorescence lifetime measurements were performed on human skin *in vivo* at an excitation wavelength of 337 nm and an emission wavelength of 460 nm. The time-resolved data were fit to a double-exponential decay, yielding lifetimes of 0.938 and 5.3 ns. The longer lifetime was attributed to the emission from collagen. The instrument was also used to measure fluorescence lifetimes of biomolecules present in human cells.

2.2 Optical Noninvasive Screening of Type 2 Diabetes

A few groups have applied spectroscopic studies to the non-invasive screening of type 2 diabetes. For example, Meerwaldt et al.³⁴ observed steady-state autofluorescence measurements of skin on the arm and lower leg of both diabetic and healthy subjects. Diabetic and healthy subjects were age- and sex-matched. Using excitation spectrum between 300 and 420 nm and emission spectrum between 420 and 600 nm, they found a positive correlation between skin autofluorescence intensity with age, diabetes duration, and mean HbA1c levels from the previous year. The fluorescence intensity also correlated well with the concentrations of AGEs in tissue biopsies, such as pentosidine and carboxymethyllysine. This demonstrated the capability of steady-state fluorescence measurements to distinguish diabetics from healthy subjects. The study's primary focus was monitoring disease progression and evaluating the patient's risk for diabetic complications. In a

later study, the same group showed that autofluorescence also correlated with severity of diabetic neuropathy³⁵ and vascular damage in type 2 diabetic subjects.³⁶ However, the effect of skin color was not addressed in these studies as nearly all subjects recruited were Caucasian. In fact, the researchers reported that data from dark-skinned subjects had to be discarded, because of nearly complete absorption of excitation light by the skin.³⁶ Otherwise, the steady-state measurements must be adjusted to account for skin complexion.

Brown et al.³⁷ clinically evaluated the use of a near-IR (NIR) spectroscopic device for its ability to correctly identify diabetic and nondiabetic subjects. The NIR wavelength region under observation in the study was from 1250 to 2500 nm. The diffusely reflected radiation was collected and the tissue absorbance was retrieved. Data from both diabetic and healthy subjects were collected and the device was found to have a sensitivity and specificity of 77.7 and 70%, respectively. Thus, this system's sensitivity and specificity are comparable to the fasting plasma glucose (FPG) test. Although a definite chemical or physiological explanation for the difference between diabetic and nondiabetic patients is yet to be elucidated, they speculate that structural changes in skin due to chronic hyperglycemia contribute to the differentiation between diabetic and nondiabetic subjects. However, the same group's previous work³⁸ suggested that NIR spectroscopy does not detect AGEs directly.

Recently, Maynard et al.³⁹ reported using a spectroscopic device for type 2 diabetes screening utilizing steady-state fluorescence as well as diffuse reflectance measurements. The fiber optic probe illuminated skin from the forearm of subjects using LED lights centered at 375, 405, 420, 435, and 460 nm. A spectrometer and CCD array then collected the light reflected and/or emitted from the skin and detected it. The spectra were corrected for skin pigmentation, hemoglobin content, and light scattering as well as age to obtain an "intrinsic" dermal fluorescence spectra. These data were then used to determine a likelihood that a subject belonged to the abnormal class, or that they were either prediabetic or diabetic. This method of screening was compared to the FPG test and A1C testing. Assuming a clinically relevant specificity of 77.4%, their method showed a sensitivity advantage of 28.8 and 17.1% versus FPG and A1C testing, respectively. The group also reported that the sensitivity of their device was not significantly different between subjects of lighter skin and those with of darker skin. Thus, their study demonstrates the promise of steady-state fluorescence for type 2 diabetes screening if factors such as skin color and age can be adjusted for in measurements. Time-resolved fluorescence may hold promise in diabetes detection by distinguishing different fluorophores emitting at the same wavelength and potentially being able to detect AGEs directly.

3 Materials and Methods

3.1 Experimental Apparatus

The study reported here made use of the TCSPC technique to measure fluorescence lifetimes of skin. A schematic of the experimental setup is shown in Fig. 1. Excitation and emission light were channeled by means of liquid light guides attached to a sensing head. Liquid light guides were used instead of commonly used fiber optics as their transmission

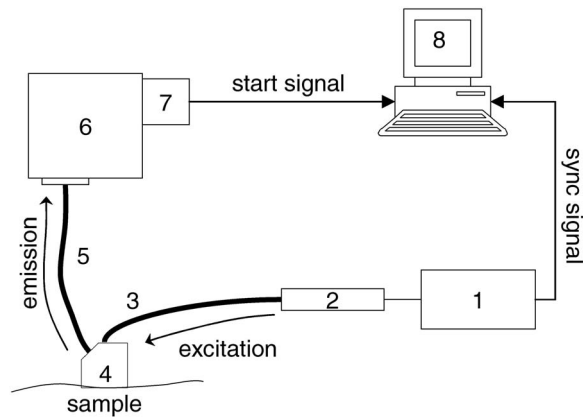


Fig. 1 Schematic of the experimental setup, including (1) diode driver, (2) LED, (3) UV liquid light guide, (4) sample probe, (5) visible liquid light guide, (6) monochromator, (7) photomultiplier tube, and (8) personal computer.

and coupling efficiency are higher compared with fiber optics. Both light guides had a diameter of 8 mm, and the excitation light guide was held 1.59 cm above the skin. The receiving end of the collection liquid light guide was held abut against the excitation liquid light guide and angled at 45 deg to the normal. The sensing head also served to shield the sample surface from ambient light. A total surface area of 6.41 cm² was exposed to excitation light.

The excitation source used was a light emitting diode or LED (PLS 370 diode, PicoQuant GmbH) with its center wavelength at 375 nm with a spectral width of around 10 nm. The full width half maximum of the diode pulses at a repetition rate of 2.5 MHz and average power of 4.8 μ W per pulse was 664 ps. The LED was driven by a diode driver (PDL-800 B diode driver, PicoQuant GmbH, Berlin, Germany) at a repetition rate of 5 MHz for all measurements, producing an estimated energy fluence rate of 2.07×10^{-6} W/cm² at the skin surface for a pulse energy of 2.65 pJ and pulse width of 664 ps. A liquid light guide designed for the UV to visible part of the spectrum (77628, from Spectra-Physics, U.S.A) carried light from the LED to the sensing head. Another liquid light guide designed for the visible part of the spectrum (77631, from Spectra-Physics, U.S.A), was used to collect the fluorescence emission and carry it to a monochromator (SpectraPro-150, Acton Research Corporation, U.S.A.). A photomultiplier tube (PMT) assembly (PMA-M 165 from PicoQuant GmbH) was coupled to the monochromator on the other end. The monochromator slits on the entry and exit of the light path were adjusted manually to maintain a bandwidth of 3 nm.

Finally, for data acquisition, the “sync” output signal from the diode driver and the “start” signal from the PMT assembly were fed to the respective channels on the data acquisition board (TimeHarp 200 from PicoQuant GmbH), via standard 50- Ω coaxial cables. The “sync” output from the diode driver provided the signal to synchronize the timing electronics on the data acquisition board mounted on a personal computer (PC). The time resolution of our device was estimated to be 200 ps.

3.2 Experimental Procedure and Parameters

The measurement procedure and parameters were arrived at by conducting preliminary studies on the palms, arms, cheeks, and feet of a 31-yr-old male Caucasian subject. The fluorescence lifetimes were measured at four different emission wavelengths: 442, 460, 478, and 496 nm. The first wavelength was chosen based on studies reporting that collagen fluorescence exhibited a maximum at around 440 nm when excited by light at 370 nm, corresponding to collagenase-digestible collagen cross-links, including AGEs on collagen.⁴⁰ The remaining wavelengths were arbitrarily chosen to cover the spectral range up to 500 nm.

To measure the fluorescence lifetimes, the monochromator was set to the emission wavelength of interest and the monochromator slits were adjusted to match that particular wavelength. The probe was then placed on the skin surface and the LED was turned on.

The PMT shutter was opened once the sensing head was firmly placed on the skin surface and then the histograms were collected using the TimeHarp software. The probe was held in contact with the palm until 1500 to 5000 counts were acquired in the peak channel. This number was arrived at by considering a trade-off between the duration of the experiments and the signal-to-noise ratio. The duration of a single measurement ranged from 5 to 20 min, based on the sensing location and emission wavelength. It was observed that the time taken for each measurement was shortest on the palm, possibly due to the low concentration of melanin. Moreover, higher emission wavelengths required longer durations to achieve these counts due to a lower intensity of the fluorescence. Figure 2 shows a typical sample of *in vivo* time-resolved fluorescence measurement on human skin along with the χ^2 and associated residuals indicating the goodness of the fit. For an acceptable fit, the χ^2 must be around 1.0 and the residuals should be randomly distributed around 0.

The instrument response function (IRF) was measured by placing the probe on a Teflon block for the same number of maximum photon counts of at least 1500 as in the *in vivo* measurements, with the PMT collecting at 403 nm. The reconvolution software FluoFit version 4.0 was used to recover the lifetimes from the measured fluorescence decays. This software utilized the Marquardt-Levenberg algorithm with a weighting factor $W(i)$ defined as

$$W(i) = 1/\sqrt{D(i)}, \quad (1)$$

where $D(i)$ is the number of counts contained in channel i . An attempt was made to describe the decays with a single-exponential, a biexponential, and a triexponential model. Only the biexponential and the triexponential models gave a value of χ^2 around 1.0, which indicated a good fit. However, the biexponential model was rejected in favor of the more complicated triexponential model due to the presence of oscillations in the plot of the residuals compared to more random residuals for the triexponential model, as illustrated in Fig. 2. Thus, the fluorescence decay could be modeled as

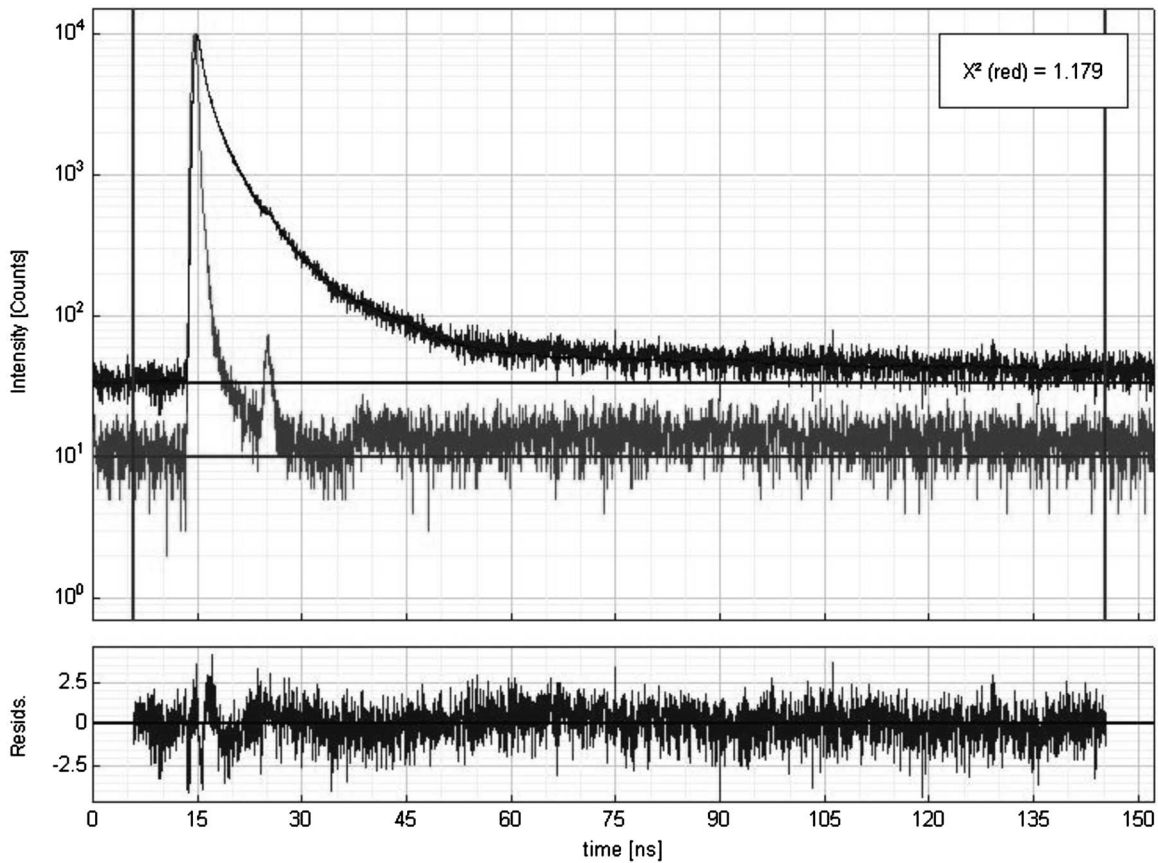


Fig. 2 Typical measurement of fluorescence decay from human skin (dark gray), IRF (light gray), and exponential decay retrieved from reconvolution (black line) with the TimeHarp Fluofit 4.0 software package.

$$F(t) = A_1 \exp(-t/\tau_1) + A_2 \exp(-t/\tau_2) + A_3 \exp(-t/\tau_3), \tag{2}$$

where A_i and τ_i are the fractional amplitude and lifetime, respectively, for decay i . Additionally, note that initial guess lifetimes were entered to enable faster convergence. A total of 75 subjects participated in this study. The population characteristics for all subjects are shown in Table 2. The palms were chosen as the sensing location for these subjects due to the shorter duration of the experiments as well as ease of access. The first measurement at 442 nm was performed on the left palm and subsequent measurements at higher wavelengths were performed alternately on the right and left palms.

In addition to time-resolved fluorescence measurements, mean HbA1c values from the previous 4 yr were recorded for diabetic subjects by obtaining medical records with Institutional Review Board (IRB) approved consent (UCLA IRB #04-12-012-02). Subjects were also recruited from the local

VA hospital with VA hospital IRB approved consent (VA IRB #PCC 2005-030449). All consent forms were signed prior to testing and collection of medical record data. All available data for each subject from the previous year were averaged and two subsets of these data were compared, one with “high” average HbA1c values and the other with “low” average HbA1c values. Data on duration of diabetes were obtained directly from the subject being tested.

4 Results and Discussion

Table 3 presents a statistical summary of lifetimes τ_1 , τ_2 , and τ_3 and the corresponding fractional amplitudes A_1 , A_2 , and A_3 for six measurements on the left palm of the same healthy subject at an emission wavelength of 442 nm. These experiments were performed over a period of 1 month at different times of the day. The coefficient of variation, which represents the variation in measurements, is less than 5% in all cases

Table 2 Population characteristics of healthy and diabetic subjects recruited for this study.

	Male/Female	Age Range (Yr)	African-American	Asian	Caucasian	Hispanic	Persian	South Asian
Healthy	22/15	10–85	4	6	18	5	2	2
Diabetic	33/5	6–80	10	1	17	10	0	0

Table 3 Statistics of fluorescence lifetimes and their corresponding amplitudes obtained from six measurements on the left palm of a 31-year-old healthy Caucasian male subject at an excitation and an emission wavelength of 375 and 442 nm, respectively.

Parameter	Mean Value	Standard Deviation	Coefficient of Variation (%)
Fluorescence Lifetime τ_1 (ns)	0.409	0.029	7.09
Amplitude A_1	0.783	0.013	1.66
Fluorescence Lifetime τ_2 (ns)	2.591	0.129	4.98
Amplitude A_2	0.183	0.008	4.37
Fluorescence Lifetime τ_3 (ns)	8.880	0.410	4.62
Amplitude A_3	0.034	0.005	14.71

except for the parameters τ_1 and A_3 , for which it reaches 7 and 15%, respectively. This shows that measurements performed with this device are highly reproducible for a single subject. Additionally, six consecutive measurements, each lasting 10 min, were performed on the same hand within an hour. No noticeable changes in lifetimes, fractional amplitudes, or acquisition times were measured, suggesting that photobleaching was not induced during the measurements.

A set of three experiments were also performed on the inner arm of the same subject over the same period of time and at an emission wavelength of 442 nm. Then, the Student's *t*-test⁴¹ was used to test differences in the fluorescence lifetimes obtained on the arm and the palm for this subject. A two-sample *t*-test assuming unequal variances was performed. In all cases, a level of significance of $p < 0.05$ was used. It was found that there were no significant differences in the fluorescence lifetime τ_1 . However, the *t*-test seemed to indicate that there was a difference in the fluorescence lifetimes τ_2 and τ_3 obtained on the arm and the palm at an emission wavelength of 442 nm. Finally, a measurement was also taken on the cheeks and the feet of the same subject. Figure 3 shows the fluorescence lifetimes τ_1 , τ_2 , and τ_3 and their corresponding fractional amplitudes A_1 , A_2 , and A_3 obtained as a function of emission wavelength and sensing location, namely, the palms, the arms, the cheeks, and the feet. The error bars in the plots of the fluorescence lifetimes represent asymptotic standard errors in the fluorescence lifetimes obtained using the Fluofit software package. Figure 3 indicates that the variations in the lifetimes from one location to another are minimal except on the cheek. Moreover, it was found in the course of the measurements that the time taken for each measurement was the least on the palm, possibly due to the low concentration of melanin. Therefore, the palm was chosen as the sensing location for all the other subjects.

Figure 4 shows the raw data of the fluorescence lifetimes and their corresponding amplitudes at an emission wavelength of 442 nm for 37 healthy subjects and 38 diabetic subjects of various ages, genders, and skin complexion obtained at the VA and UCLA. The error bars represent asymptotic standard errors in the fluorescence lifetimes obtained using the Fluofit software package. To further analyze the fluorescence lifetime data, various factors varying from one individual to another

were considered, namely, (1) skin complexion (2) gender, and (3) age. The statistical analysis used was the Student's *t*-test assuming unequal variance. Based on this test, a two-tailed *p* value, defined as the probability that the difference between two groups randomly occurred during the experiment, was assumed to be statistically significant.

4.1 Effect of Skin Complexion and Gender

Figure 5 shows the fluorescence lifetimes τ_1 , τ_2 , and τ_3 and their corresponding amplitudes A_1 , A_2 , and A_3 as a function skin complexion for healthy subjects at an emission wavelength of 442 nm. The figure indicates that the fluorescence lifetimes do not significantly vary for different skin complexions. Using the Fisher's exact test,⁴¹ the fluorescence lifetimes and fractional amplitudes of healthy subjects with dark complexion and light complexion were compared. The light-complexioned group consisted of 10 Caucasian subjects, age 42 ± 12 yr, while the dark-complexioned group was composed of 10 Hispanic, Persian, South Asian, and African-American subjects, age 39 ± 20 yr. Based on these test results, no statistically significant difference in average fluorescence lifetimes and fractional amplitudes exists between these two groups ($p > 0.05$ in all cases). Note that measurements took longer for dark skin. However, skin complexion had no effect on the lifetimes and fractional amplitudes.

Moreover, Fig. 6 shows the fluorescence lifetimes and amplitudes as a function of gender for healthy subjects in the same age group at the same emission wavelength of 442 nm. Again, there are no noticeable trends in the fluorescence lifetimes with respect to gender. The comparison of the fluorescence lifetimes and fractional amplitudes of 15 healthy female subjects, average age 42 ± 12 yr, and 22 healthy male subjects, average age 48 ± 20 yr, did not produce statistically significant differences ($p > 0.05$ for all cases). Thus, Figs. 5 and 6 as well as the statistical analysis suggest that fluorescence lifetimes and fractional amplitudes do not vary with skin complexion and gender. The same conclusions were made for other emission wavelengths (data not shown).

4.2 Effect of Age

Finally, an attempt was made to model the fluorescence lifetimes of healthy subjects shown in Fig. 4 as a function of age using linear regression. The square of the correlation coefficient R^2 was less than 0.03 for all three lifetimes, thus indicating that variations in fluorescence lifetimes with age cannot be described by a linear model (data not shown). Moreover, the small regression coefficients in all the cases also indicate that the three lifetimes do not depend on the age of the subject. Student's *t*-tests were performed on all six parameters (fluorescence lifetimes and fractional amplitudes) comparing young and old healthy subjects. In addition, 15 subjects in both the young and old groups were compared with average ages of 31 ± 7 and 63 ± 11 yr, respectively. No statistically significant difference was detected for any of the parameters ($p > 0.05$). Thus, the lifetimes and fractional amplitudes obtained for healthy subjects are statistically independent of age, gender, and skin complexion. Table 4 presents the mean values and the standard deviations of the fluorescence lifetimes and their corresponding fractional amplitudes for healthy subjects, providing reference values for healthy human skin. This

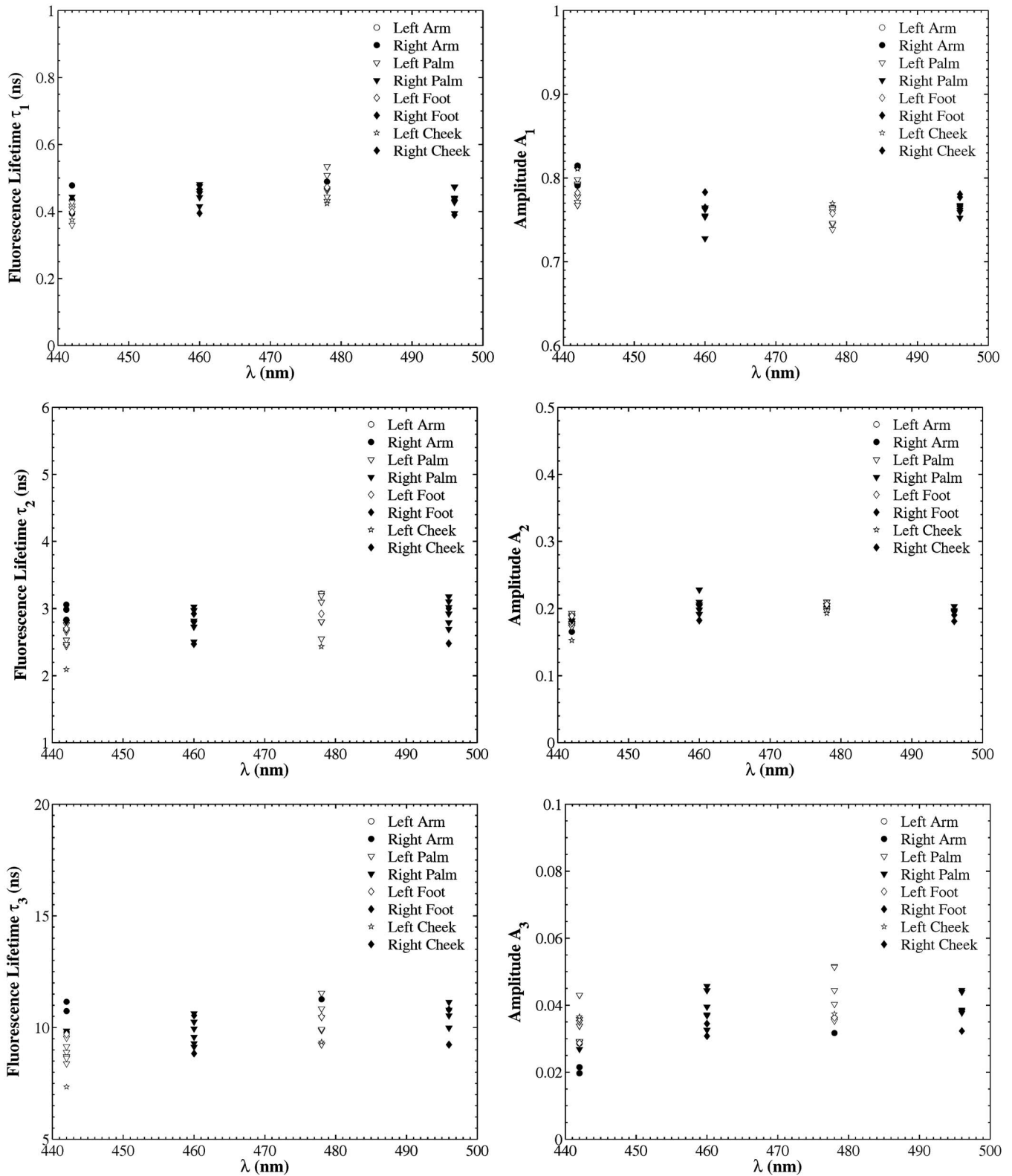


Fig. 3 Effect of sensing location on fluorescence lifetimes τ_1 , τ_2 , and τ_3 and fractional amplitudes A_1 , A_2 , and A_3 as a function of emission wavelength for a 31-year-old Caucasian male subject at excitation wavelength of 375 nm.

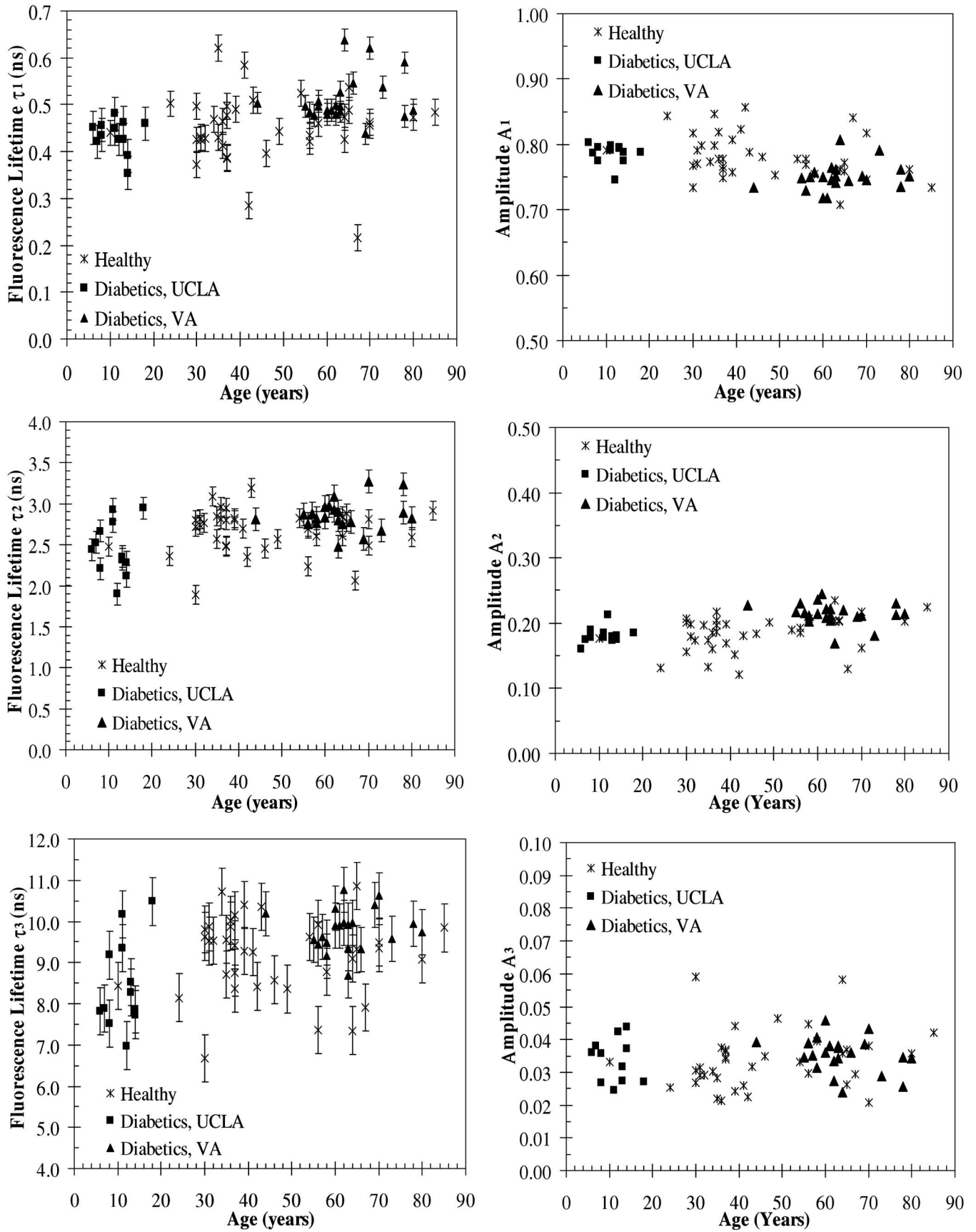


Fig. 4 Effect of age on the fluorescence lifetimes τ_1 , τ_2 , and τ_3 and fractional amplitudes A_1 , A_2 , and A_3 for healthy and diabetic subjects at excitation and emission wavelengths of 375 nm and 442 nm, respectively.

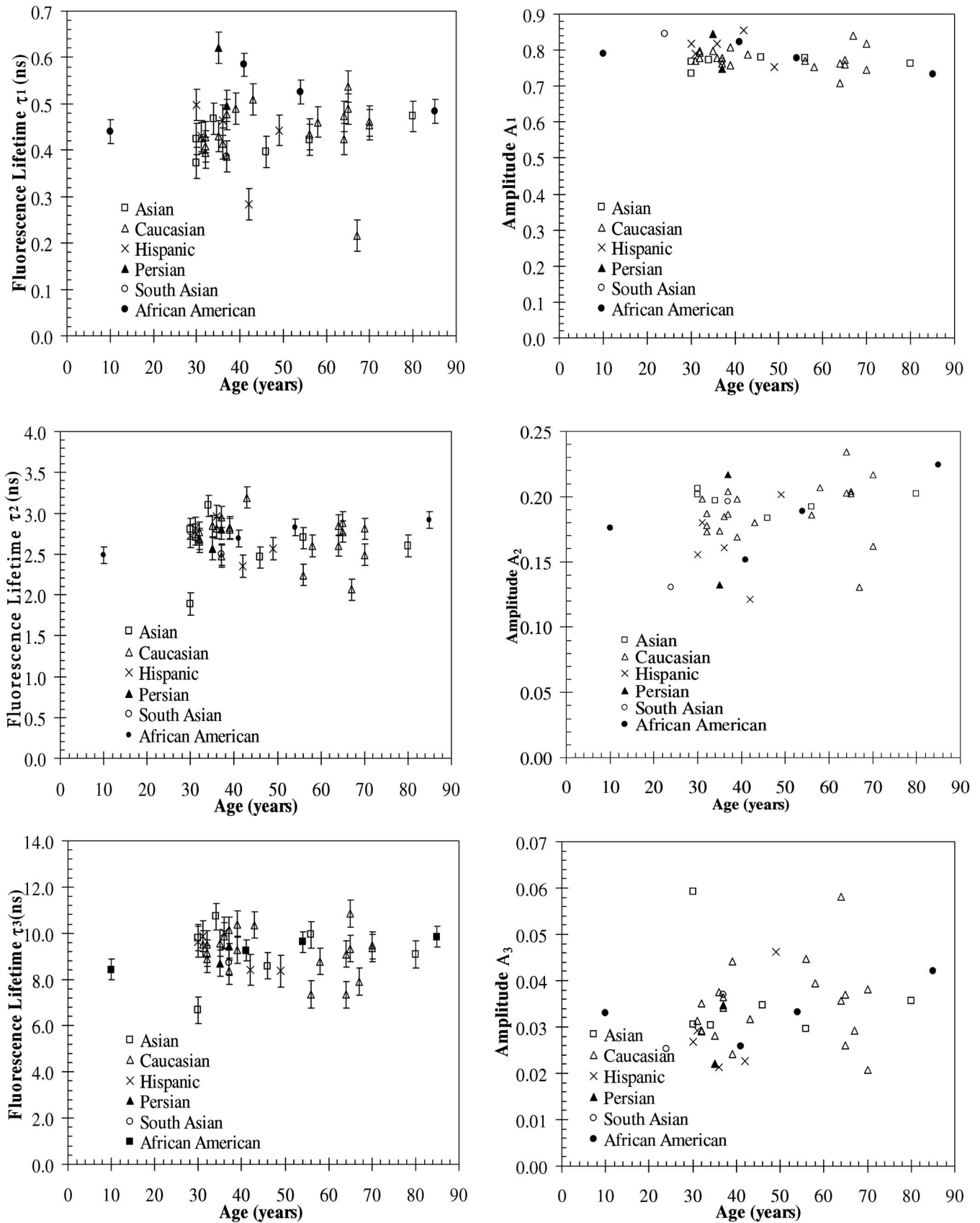


Fig. 5 Effect of skin complexion on the fluorescence lifetimes τ_1 , τ_2 , and τ_3 and fractional amplitudes A_1 , A_2 , and A_3 as a function of age for healthy subjects at excitation and emission wavelengths of 375 nm and 442 nm, respectively.

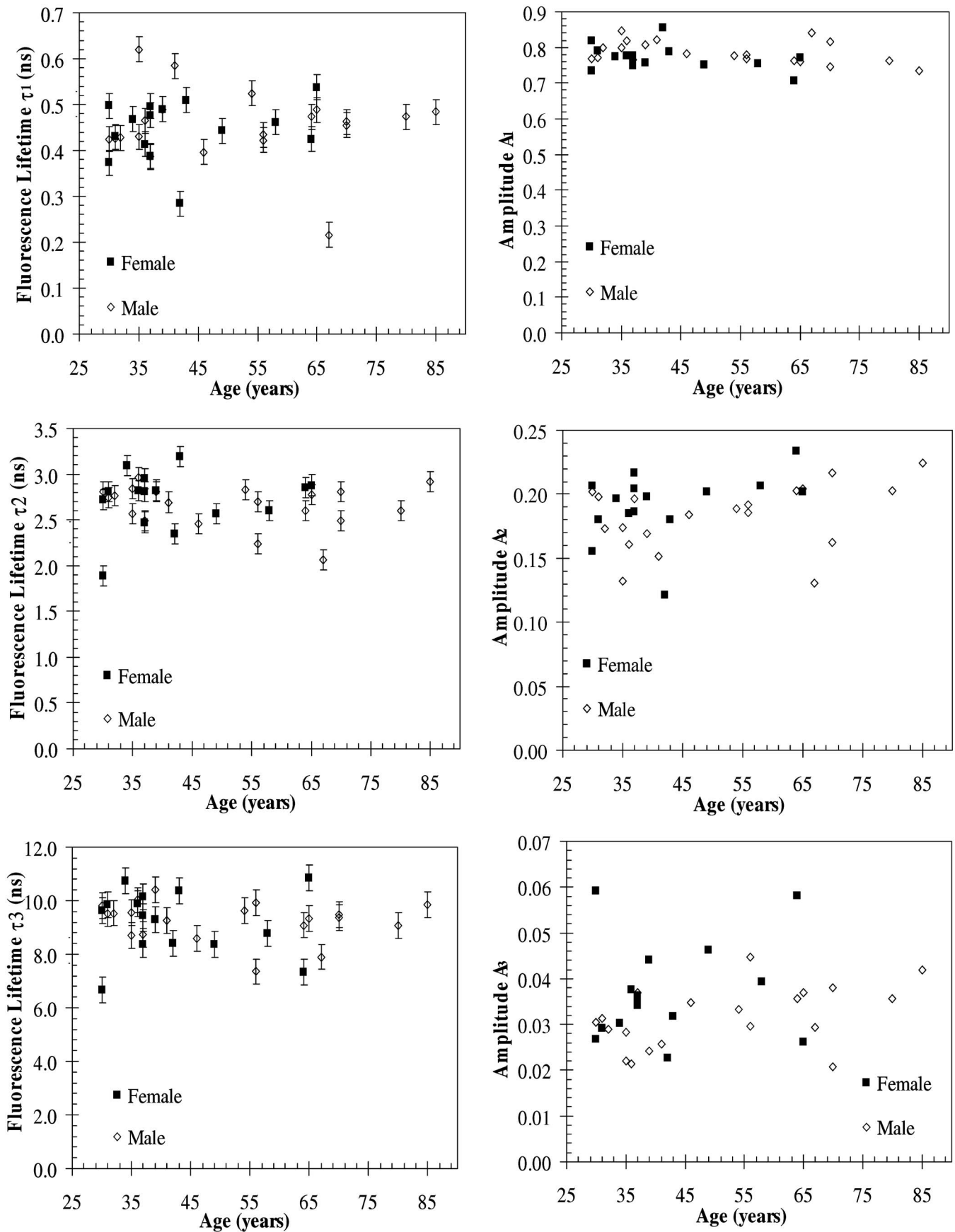


Fig. 6 Effect of gender on the fluorescence lifetimes τ_1 , τ_2 , and τ_3 and fractional amplitudes A_1 , A_2 , and A_3 as a function of age for healthy subjects at an excitation and emission wavelengths of 375 nm and 442 nm, respectively.

Table 4 Statistics of the decay parameters obtained on the left palm of 18 healthy and 27 diabetic subjects at an emission wavelength of 442 nm; the reported *p* values were obtained using the unpaired Student's *t*-test to compare healthy and diabetic populations.

Parameter	Group	Mean Value	Variance	<i>p</i> value
Fluorescence Lifetime τ_1 (ns)	Healthy	0.477	0.002	
	Diabetic	0.504	0.003	0.07
Amplitude A_1	Healthy	0.769	0.0008	
	Diabetic	0.749	0.0004	0.01
Fluorescence Lifetime τ_2 (ns)	Healthy	2.74	0.05	
	Diabetic	2.82	0.06	0.21
Amplitude A_2	Healthy	0.196	0.0004	
	Diabetic	0.215	0.0002	0.002
Fluorescence Lifetime τ_3 (ns)	Healthy	9.35	0.85	
	Diabetic	9.79	0.61	0.10
Amplitude A_3	Healthy	0.035	0.0001	
	Diabetic	0.036	0.0001	0.72

clearly demonstrates the advantage of time-resolved fluorescence over steady-state fluorescence in that it is insensitive to age and skin complexion.

4.3 Effect of Diabetes

Table 4 summarizes the experimental data collected for 18 healthy subjects and 27 age-matched diabetic subjects. Their fluorescence lifetimes and fractional amplitudes were compared by means of an unpaired Student's *t*-test. Only the fractional amplitudes A_1 and A_2 produced statistically significant differences in the means of the diabetic and the healthy patients. This was based on the criteria that $p < 0.05$ for the difference between average values to be considered significant. Additionally, the relative contributions of each lifetime to the overall intensity of diabetic and healthy subjects were compared using the Student's *t*-test. The fractional contribution of a single lifetime to the steady-state intensity can be defined as⁴

$$I_i = (\tau_i A_i) / \sum_{i=1}^n (\tau_i A_i). \quad (3)$$

However, no statistically significant differences were found for any of the three fluorescence lifetimes considered. The same conclusions were reached for the other emission wavelengths considered (data not shown).

Further testing was performed on only the diabetic subjects, comparing duration of diabetes as well as average HbA1c values over the past 4 yr. To test the effect of diabetes

Table 5 Statistics of the decay parameters on the left palm of 18 diabetic subjects with foot ulcers and 18 age-matched healthy subjects at an emission wavelength of 442 nm; the reported *p* values were obtained using the unpaired Student's *t*-test to compare healthy and diabetic populations.

Parameter	Group	Mean Value	Variance	<i>p</i> value
Fluorescence Lifetime τ_1 (ns)	Healthy	0.477	0.002	
	Diabetic with foot ulcers	0.510	0.002	0.038
Amplitude A_1	Healthy	0.769	0.001	
	Diabetic with foot ulcers	0.761	0.0003	0.012
Fluorescence Lifetime τ_2 (ns)	Healthy	2.73	0.05	
	Diabetic with foot ulcers	2.86	0.03	0.05
Amplitude A_2	Healthy	0.196	0.0003	
	Diabetic with foot ulcers	0.217	0.0004	0.002
Fluorescence Lifetime τ_3 (ns)	Healthy	9.34	0.85	
	Diabetic with foot ulcers	9.81	0.24	0.07
Amplitude A_3	Healthy	0.036	0.0001	
	Diabetic with foot ulcers	0.035	0.0001	0.91

duration, the diabetic subjects were divided into two groups with an average of 11 ± 5 yr since diagnosis in the shorter duration group and 24 ± 7 yr in the longer duration group. However, no statistically significant difference was found between these two groups when performing the unpaired Student's *t*-test. Similarly, any correlation with average HbA1c from the previous 4 yr was tested by dividing the diabetic subjects into two groups: one with a low average HbA1c of $6.9 \pm 0.7\%$ and higher average HbA1c of $9.8 \pm 0.9\%$. No significant difference was detected between these two groups ($p > 0.05$ for all cases).

Additionally, 18 diabetic subjects with foot ulcers, aged 62 ± 8 yr, were compared with 18 age-matched healthy subjects, average age 57 ± 15 yr, using the Student's *t*-test. Diabetic subjects with foot ulcers were specifically chosen because many diabetic subjects who develop ulcers also have other comorbidities associated with diabetes.^{42,43} Thus, this group represents subjects whose AGE accumulation is expected to be much higher than other diabetic subjects. Not only were statistically significant differences noted between the two groups for fractional amplitudes A_1 and A_2 , but also differences in lifetime τ_1 between the two groups was also statistically significant, albeit with a *p* value of 0.038. All the test results are presented in Table 5. Given the long half-life of collagen in skin⁴⁴ (~ 15 yr), one can expect changes in the time-resolved fluorescence properties of skin to correlate more with the occurrence of diabetic complications than with HbA1c values. This measurement would indicate the long-

term accumulation of AGEs and other oxidative damage. The rate at which tissue accumulates AGEs is also dependent on various genetic or metabolic factors.⁴⁵ Therefore, not all diabetic subjects are as susceptible to the development of complications, in spite of poor blood glucose control and high HbA1c levels. The development of complications cannot be predicted by conventional treatment monitoring such as blood glucose measurements and HbA1c tests. Finally, nine diabetic subjects without foot ulcers were compared with 18 age-matched healthy subjects using the Student's *t*-test. No statistically significant differences between the two groups were detected in any of the parameters except in amplitude A_2 (p value of 0.045). This indicates that the differences in the amplitude A_1 and τ_1 between 18 healthy and 27 diabetic subjects reported earlier might be mainly due to the diabetic subjects with foot ulcers.

While a previous study by Meerwaldt et al.³⁴ showed that steady-state autofluorescence measurements correlated with age, diabetes duration, and mean HbA1c of the previous year, this study did not find any significant relationships between the fluorescence lifetimes and amplitudes and these variables. Meerwaldt et al.³⁴ used a polychromatic excitation source emitting at wavelengths ranging from 300 to 420 nm and fluorescence was measured over the entire window of 420 to 600 nm. This is in contrast with this study, where the excitation source was a monochromatic diode emitting at 375 nm (spectral width of around 10 nm) and fluorescence was measured at 442, 460, 478, and 496 nm with spectral width of 3 nm. It is speculated that these differences in the excitation wavelength might be the source of the different conclusions obtained in the two studies. This study should be repeated for a different excitation wavelength between 300 and 420 nm and emission wavelength between 420 and 600 nm to corroborate results by Meerwaldt et al.³⁴

4.4 Identification of Fluorophores

In an earlier study on fluorescence lifetime measurements on human skin,³³ two fluorescence lifetimes of 0.4 and 2.4 ns at the stratum spinosum were reported using multiphoton excitation at 740 nm, equivalent to single-photon excitation at 370 nm. In the presented study, similar values were found when the decays were fit to a triexponential model. This suggests that the fluorophores with the high fractional amplitudes A_1 and A_2 in our measurements originate, at least in part, from the stratum spinosum. Our measurements are detecting another fluorophore as well, perhaps deeper in the tissue, which would explain the lower contribution of this fluorophore to the overall fluorescence signal. The similarities between our results and the previously reported data help to validate our results in spite of using different multiexponential models. Moreover, the shorter two lifetimes τ_1 around 0.4 ns and τ_2 around 2.7 ns observed in our measurements were similar to the lifetimes of free and protein-bound NADH reported in literature.^{31,46} Indeed, Schneckenburger et al.⁴⁶ studied the autofluorescence from cultivated endothelial cells and determined the fluorescence lifetime of free and protein-bound NADH to be between 0.4 and 0.5 and between 2.0 to 2.5 ns, respectively. In addition, König and Riemann³¹ also reported a fluorescence lifetime of 2.7 ns at a depth of 50 μm within the skin, which could possibly be attributed to bound NADH.

Based on these studies, it is speculated that the two shorter fluorescence lifetimes τ_1 and τ_2 correspond to free and protein-bound NADH, respectively. This suggests that the differences in fractional amplitudes A_1 and A_2 observed between diabetic and healthy subjects are related to the metabolic states of their tissues rather than directly detecting the presence of glycation products. However, as the presence of glycation products is known to increase tissue oxidative stress,^{47,48} they may have an indirect effect on our measurements.

Furthermore, it is speculated that the third observed average lifetime τ_3 equal to 9.2 ns for healthy subjects corresponds to collagen cross-links formed^{34,38} by AGEs. However, our data on diabetic subjects seem to contradict this speculation. The longest lifetime τ_3 and the corresponding fractional amplitude A_3 are not significantly different between diabetic and healthy subjects. Given the known correlation between AGEs and diabetes and skin steady-state autofluorescence,³⁴ one would expect the fractional amplitude of the third lifetime to increase with increasing AGE accumulation, if the lifetime could be attributed to AGEs. With elevated concentration of AGEs in the skin, their fluorescence signal would be stronger and, thus, contribute a higher fractional intensity. Further *in vitro* experimentation is required to precisely determine the origin of this lifetime.

5 Conclusions

We presented the design and implementation of an experimental apparatus based on TCSPC assembled to measure autofluorescence lifetimes of human skin. With an excitation wavelength of 375 nm and pulse width of 700 ps, fluorescence was detected at wavelengths of 442, 460, 478, and 496 nm. The device was tested on various locations of a 31-yr-old healthy male Caucasian subject as well as the palms of 37 healthy subjects and 38 diabetic subjects. The following conclusions were drawn:

1. In tests on all subjects, the fluorescence decay was fit to a multiexponential model with three average fluorescence lifetimes of 0.5, 2.6, and 9.2 ns and associated average fractional amplitudes of 0.78, 0.18, and 0.03, respectively, for nondiabetic subjects.
2. A statistical analysis of the fluorescence lifetimes obtained on the inner arm, palm, feet, and the cheeks of a 31-yr-old healthy male Caucasian subject showed differences between sensing locations for τ_1 and τ_3 , while there were no differences in τ_1 .
3. It was found that the fluorescence lifetimes measured on the palms were independent of the skin complexion and the gender of the subjects.
4. The only statistically significant differences between diabetic and nondiabetic subjects were between fractional amplitudes A_1 and A_2 of the two groups.
5. No differences in any parameters were observed between subjects due to HbA1c values or diabetes duration.
6. A comparison between diabetic subjects with foot ulcers and healthy subjects showed statistically significant differences not only in fractional amplitudes A_1 and A_2 , but also in lifetime τ_1 .
7. Finally, the only parameter that showed a statistically significant difference between the diabetic subjects without

foot ulcers and age-matched healthy subjects was A_2 .

The fluorescence lifetime data of healthy subjects is of particular interest as a baseline especially for using fluorescence lifetimes of NADH to noninvasively sense glucose concentrations¹⁴ as well as monitoring diseases and skin conditions such as skin cancer, wounds, and ulcers.

Acknowledgments

The authors would like to thank Dr. Mark Elliot for insightful discussion and Evon Fanous for her help at the Veteran's Administration, Los Angeles. This work was supported by UCLA Office of Intellectual Property Administration, UCLA Faculty Senate Grant, and by the Diabetes Action Research and Education Foundation.

References

1. R. Richards-Kortum and E. Sevick-Muraca, "Quantitative optical spectroscopy for tissue diagnostics," *Annu. Rev. Phys. Chem.* **47**, 555–606 (1996).
2. J. D. Pitts and M.-A. Mycek, "Design and development of a rapid acquisition laser-based fluorometer with simultaneous spectral and temporal resolution," *Rev. Sci. Instrum.* **72**, 3061–3072 (2001).
3. Q. Fang, T. Papaioannou, J. A. Jo, R. Vaitha, K. Shastry, and L. Marcu, "Time-domain laser-induced fluorescence spectroscopy apparatus for clinical diagnostics," *Rev. Sci. Instrum.* **75**(1), 151–162 (2004).
4. J. R. Lakowicz, *Principles of Fluorescence Spectroscopy*, Kluwer Academic/Plenum Publishers, New York (1999).
5. American Diabetes Association, "Economic costs of diabetes in the U.S. in 2002," *Diabetes Care* **26**, 917–932 (2003).
6. American Diabetes Association, "Diagnosis and classification of diabetes mellitus," *Diabetes Care* **29**(Suppl.1), S43–S48 (2006).
7. M. Engelgau, K. Narayan, and H. W. H., "Screening for type 2 diabetes," *Diabetes Care* **23**, 1563–1580 (2000).
8. D. B. Sacks, D. E. Bruns, D. E. Goldstein, N. K. Maclaren, J. M. McDonald, and M. Parrott, "Guidelines and recommendations for laboratory analysis in the diagnosis and management of diabetes mellitus," *Clin. Chem.* **48**, 436–472 (2002).
9. R. Singh, A. Barden, T. Mori, and L. Beilin, "Advanced glycation end-products: a review," *Diabetologia* **44**, 129–146 (2001).
10. R. Na, I. Stender, M. Henrikson, and H. Wulf, "Autofluorescence of human skin is age-related when corrected for skin-pigmentation and redness," *J. Invest. Dermatol.* **116**, 536–540 (2001).
11. D. Sell, R. Nagaraj, S. Grandhee, P. Odetti, A. Lapolla, J. Fogarty, and V. Monnier, "Pentosidine: a molecular marker for the cumulative damage due to proteins in diabetes, aging and uremia," *Diabetes/Metab. Rev.* **7**(4), 239–251 (1991).
12. V. Monnier, G. Mustata, K. Beimeil, O. Reihl, M. Lederer, D. Zhenyu, and D. Sell, "Cross-linking of the extracellular matrix by the Maillard reaction in aging and diabetes," *Ann. N.Y. Acad. Sci.* **1043**, 533–544 (2005).
13. M. Meli, R. Granouillet, E. Reynaud, A. Chamson, J. Frey, and C. Perier, "In vitro glycooxidation of insoluble fibrous type I collagen: solubilization and advanced glycation end products," *J. Protein Chem.* **22**(6), 527–531 (2003).
14. N. Evans, L. Gnudi, O. Rolinski, D. Birch, and J. Pickup, "Glucose-dependent changes in NAD(P)H-related fluorescence lifetime of adipocytes and fibroblasts in vitro: potential for non-invasive glucose sensing in diabetes mellitus," *J. Photochem. Photobiol., B* **80**(2), 122–129 (2005).
15. D. P. O'Neal, M. J. McShane, M. V. Pishko, and G. L. Cote, "Implantable biosensors: if analysis of fluorescent light propagation through skin," in *Optical Diagnostics and Sensing of Biological Fluids and Glucose and Cholesterol Monitoring Proc. SPIE* **4263**(1), 20–24 (2001).
16. A. Pradhan, B. B. Das, K. M. Yoo, R. R. Alfano, J. Cleary, R. Prudente, and E. J. Celmer, "Time-resolved fluorescence of benign and malignant breast tissues," *Proc. SPIE* **1599**(1), 81–84 (1992).
17. T. M. Glanzmann, J.-P. Ballini, P. Jichlinski, H. van den Bergh, and G. A. Wagnieres, "Tissue characterization by time-resolved fluorescence spectroscopy of endogenous and exogenous fluorochromes: apparatus design and preliminary results," *Proc. SPIE* **2926**, 41–50 (1996).
18. T. Glanzmann, J.-P. Ballini, H. van den Bergh, and G. Wagnieres, "Time-resolved spectrofluorometer for clinical tissue characterization during endoscopy," *Rev. Sci. Instrum.* **70**, 4067–4077 (1999).
19. T. M. Glanzmann, P. Uehlinger, J.-P. Ballini, A. Radu, T. Gabrecht, P. Monnier, H. van den Bergh, and G. A. Wagnieres, "Time-resolved autofluorescence spectroscopy of the bronchial mucosa for the detection of early cancer: clinical results," *Proc. SPIE* **4432**, 199–209 (2001).
20. J. Mizeret, T. Stepinac, M. Hansroul, A. Studzinski, H. van den Bergh, and G. Wagnieres, "Instrumentation for real-time fluorescence lifetime imaging in endoscopy," *Rev. Sci. Instrum.* **70**, 4689–4701 (1999).
21. T. J. Pfeifer, D. Y. Paithankar, J. M. Poneros, K. T. Schomacker, and N. S. Nishioka, "Temporally and spectrally resolved fluorescence spectroscopy for the detection of high grade dysplasia in Barrett's esophagus," *Lasers Surg. Med.* **32**(1), 10–16 (2003).
22. D. Schweitzer, A. Kolb, M. Hammer, and E. Thamm, "Tau-mapping of the autofluorescence of the human ocular fundus," *Proc. SPIE* **4164**, 79–89 (2000).
23. D. Schweitzer, A. Kolb, and M. Hammer, "Autofluorescence lifetime measurements in images of the human ocular fundus," *Proc. SPIE* **4432**, 29–39 (2001).
24. D. Schweitzer, M. Hammer, F. Schweitzer, R. Anders, T. Doebbecke, S. Schenke, E. R. Gaillard, and E. R. Gaillard, "In vivo measurement of time-resolved autofluorescence at the human fundus," *J. Biomed. Opt.* **9**(6), 1214–1222 (2004).
25. J.-M. I. Maarek, L. Marcu, M. C. Fishbein, and W. S. Grundfest, "Time-resolved fluorescence of human aortic wall: use for improved identification of atherosclerotic lesions," *Lasers Surg. Med.* **27**, 241–254 (2000).
26. L. Marcu, W. S. Grundfest, and J.-M. I. Maarek, "Arterial fluorescent components involved in atherosclerotic plaque instability: differentiation by time-resolved fluorescence spectroscopy," *Proc. SPIE* **4244**, 428–433 (2001).
27. R. Cubeddu, A. Pifferi, P. Taroni, A. Torricelli, G. Valentini, and E. Sorbellini, "Fluorescence lifetime imaging: an application to the detection of skin tumors," *IEEE J. Sel. Top. Quantum Electron.* **5**(4), 122–132 (1999).
28. R. Cubeddu, D. Comelli, C. D'Andrea, P. Taroni, and G. Valentini, "Clinical system for skin tumour detection by fluorescence lifetime imaging," *IEEE Eng. Med. Biol. Mag.* **3**, 2295–2296 (2002).
29. J. Siegel, D. S. Elson, S. E. D. Webb, K. C. B. Lee, A. Vlandas, G. L. Gamaruto, S. L. Fort, M. J. Lever, P. J. Tadrous, G. W. H. Stamp, A. L. Wallace, A. Sandison, T. F. Watson, F. Alvarez, and P. M. W. French, "Studying biological tissue with fluorescence lifetime imaging: microscopy, endoscopy, and complex decay profiles," *Appl. Opt.* **42**(16), 2995–3004 (2003).
30. K. Koenig, U. Wollina, I. Riemann, C. Peukert, K.-J. Halbhuber, H. Konrad, P. Fischer, V. Fuenfstueck, T. W. Fischer, and P. Elsner, "Optical tomography of human skin with subcellular spatial and picosecond time resolution using intense near infrared femtosecond laser pulses," *Proc. SPIE* **4620**, 191–201 (2002).
31. K. Konig and I. Riemann, "High-resolution multiphoton tomography of human skin with subcellular spatial resolution and picosecond time resolution," *J. Biomed. Opt.* **8**(3), 432–439 (2003).
32. I. Riemann, E. Dimitrov, P. Fischer, A. Reif, M. Kaatz, P. Elsner, and K. Konig, "High-resolution multiphoton tomography of human skin in vivo and in vitro," *Proc. SPIE* **5463**, 21–28 (2004).
33. A. Ehlers, I. Riemann, T. Anhut, M. Kaatz, P. Elsner, and K. Konig, "Fluorescence lifetime imaging of human skin and hair," *Proc. SPIE* **6089**, N1–N10 (2006).
34. R. Meerwaldt, R. Graaff, P. H. N. Oomen, T. P. Links, J. J. Jager, N. L. Alderson, S. R. Thorpe, J. W. Baynes, R. O. B. Gans, and A. J. Smit, "Simple non-invasive assessment of advanced glycation end-product accumulation," *Diabetologia* **47**, 1324–1330 (2004).
35. R. Meerwaldt, T. P. Links, R. Graaff, K. Hoogenberg, J. D. Lefrandt, J. W. Baynes, R. O. B. Gans, and A. J. Smit, "Increased accumulation of skin advanced glycation end-products precedes and correlates with clinical manifestation of diabetic neuropathy," *Diabetologia* **48**, 1637–1644 (2005).

36. H. L. Lutgers, H. J. Bilo, R. Graaff, R. O. Gans, T. P. Links, A. J. Smit, and L. J. Ubink-Veltmaat, "Skin autofluorescence as a noninvasive marker of vascular damage in patients with type 2 diabetes," *Diabetes Care* **29**(12), 2654–2659 (2006).
37. C. Brown, H. Davis, M. Ediger, C. Fleming, E. Hull, and M. Rohrscheib, "Clinical assessment of near-infrared spectroscopy for noninvasive diabetes screening," *Diabetes Technol. Ther.* **7**(3), 456–466 (2005).
38. E. Hull, M. Ediger, A. Unione, E. Deemer, M. Stroman, and J. Baynes, "Noninvasive, optical detection of diabetes: model studies with porcine skin," *Opt. Express* **12**(19), 4496–4510 (2004).
39. J. Maynard, M. Rohrscheib, J. Way, C. M. Nguyen, and M. N. Ediger, "Noninvasive type 2 diabetes screening: superior sensitivity to fasting plasma glucose and alc," *Diabetes Care* **30**(5), 1120–1124 (2007).
40. R. H. Na, I. M. Stender, M. Henriksen, and H. C. Wulf, "Autofluorescence of human skin is age-related after correction for skin pigmentation and redness," *J. Invest. Dermatol.* **116**, 536–540 (2001).
41. S. Glantz, *Primer of Biostatistics*, McGraw-Hill, New York (2002).
42. R. Nelson, D. Gohdes, J. Everhart, J. Hartner, F. Zwemer, D. Pettitt, and W. Knowler, "Lower-extremity amputations in NIDDM: 12-yr follow-up study in Pima Indians," *Diabetes Care* **11**(1), 8–16 (1988).
43. G. Reiber, R. Pecoraro, and T. Koepsell, "Risk factors for amputation in patients with diabetes mellitus. a case control study," *Ann. Intern Med.* **117**(2), 97–105 (1992).
44. N. Verzijl, J. DeRoot, S. Thorpe, R. A. Bank, J. N. Shaw, T. J. Lyons, J. W. J. Bijlsma, F. P. J. G. Lafeber, J. W. Baynes, and J. M. TeKoppele, "Effect of collagen turnover on the accumulation of advanced glycation end products," *J. Biol. Chem.* **275**(50), 39027–39031 (2000).
45. H. Vlassara and M. Palace, "Diabetes and advanced glycation end-products," *J. Intern Med.* **251**(2), 87–101 (2002).
46. H. Schneckenburger, M. Wagner, P. Weber, W. S. Strauss, and R. Sailer, "Autofluorescence lifetime imaging of cultivated cells using a UV picosecond laser diode," *J. Fluoresc.* **14**(5), 649–654 (2004).
47. T. Wendt, N. Tanji, J. Guo, B. Hudson, A. Bierhaus, R. Ramasamy, B. Arnold, P. Nawroth, S. F. Yan, V. D'Agati, and A. Schmidt, "Glucose, glycation and RAGE: implication for amplification of cellular dysfunction in diabetic nephropathy," *J. Am. Soc. Nephrol.* **14**(5), 1383–1395 (2003).
48. J. W. Baynes and S. R. Thorpe, "Role of oxidative stress in diabetic complications: a new perspective on an old paradigm," *Diabetes* **48**(1), 1–9 (1999).